DED2 68

NATURE, VOL. 217, JANUARY 13, 1968

Reconstruction of Three Dimensional Structures from Electron Micrographs

by

D. J. DE ROSIER
A. KLUG

MRC Laboratory of Molecular Biology, Hills Road, Cambridge

General principles are formulated for the objective reconstruction of a three dimensional object from a set of electron microscope images. These principles are applied to the calculation of a three dimensional density map of the tail of bacteriophage *T4*.

THE standard high resolution electron microscope has a depth of focus of several thousand Ångströms, making the image a two dimensional superposition of different levels in the three dimensional structure. The focus cannot be adjusted to different levels within the object, and so three dimensional structures are difficult to analyse. Stereo-electron micrographs do not overcome this difficulty satisfactorily, as will be shown.

Our method starts from the obvious premise that more than one view is generally needed to see an object in three dimensions. We determine first the number of views required for reconstructing an object to a given degree of resolution and find a systematic way of obtaining these views. The electron microscope images corresponding to these different views are then combined mathematically, by a procedure which is both quantitative and free from arbitrary assumptions, to give the three dimensional structure in a tangible and permanent form. The method is most powerful for objects containing symmetrically arranged subunits, for here a single image effectively contains many different views of the structure. The symmetry of such an object can be introduced into the process of reconstruction, allowing the three dimensional structure to be reconstructed from a single view, or a small number of views. In principle, however, the method is applicable to any kind of structure, including individual, unsymmetrical particles, or sections of biological specimens.

Summary of Procedure

Electron micrographs are selected in which the details of the structure show up best, as judged for example in the phage tail described later, by their optical diffraction patterns[1,2]. The optical density in each image is sampled at regular points on a grid by an automatic microdensitometer linked to a computer (unpublished work of U. W. Arndt, R. A. Crowther and J. F. W. Mallett), which converts the image into a set of numbers representing the density at each grid point. These numbers are now transformed by computation into a set of Fourier

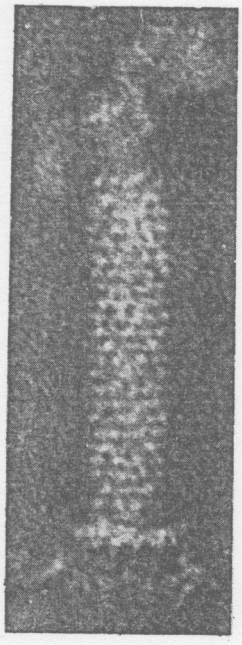

Fig. 1

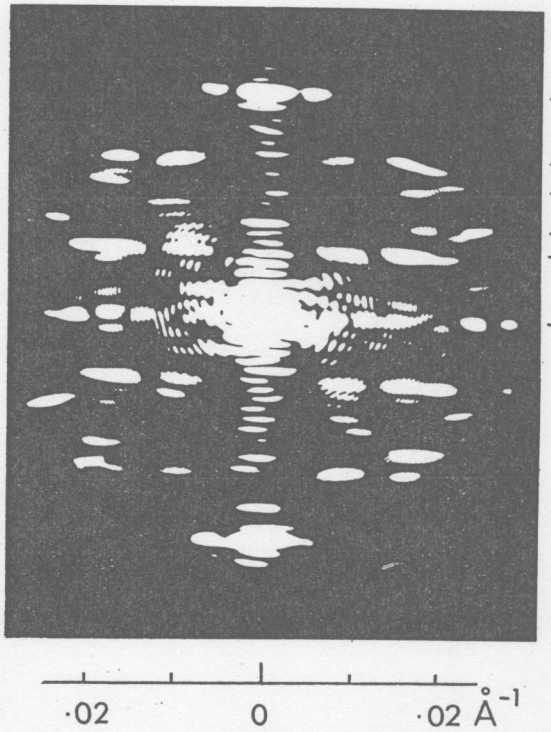

Fig. 2

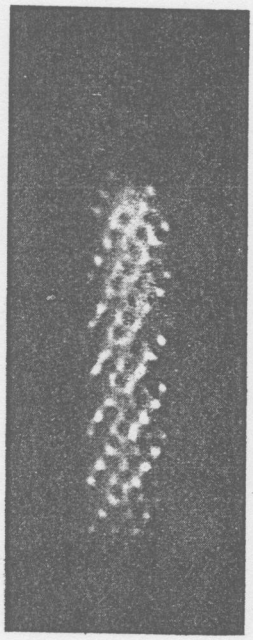

Fig. 3

Fig. 1. Electron micrograph of a tail of bacteriophage *T4*, negatively stained with uranyl formate. (× 500,000.)

Fig. 2. Optical diffraction pattern of the phage tail image in Fig. 1. Stronger exposures show that the order in the micrograph extends to spacings of about 25 Å. The strong meridional peak on the seventh layer line arises from the spacing of 38 Å between annuli. The layer lines are approximately equally spaced at the orders of an approximate repeat of $7 \times 38 = 266$ Å. The helical selection rule for the diffraction pattern is $l = 2n + 7m$, the only permitted values of n being those which are multiples of six.

Fig. 3. Optically filtered image of phage tail in Fig. 1, admitting only the diffracted rays corresponding to the far side of the particle. The dominant features are two distinct sets of oblique striations, which correspond to two distinct sets of helical lines running along two cylindrical surfaces of different diameter, and thus correspond to features at different depths in the particle.

amplitudes and phases*. A Fourier synthesis is then carried out which takes into account the symmetry of the object† and which builds up a three dimensional map of the structure. The density at each point on this map is made up by the summation of Fourier components contributed by all the different images of the object. This final step is similar to the method which is used by crystallographers for building up three dimensional maps of molecules from the amplitudes and phases of the X-rays diffracted by a crystal. The X-ray diffraction pattern lacks information about the phases, but these are readily calculated here from the density distribution in the original electron micrographs‡.

Application to the Tail of Bacteriophage T4

The tail of the *T*-even bacteriophages is made up of a core surrounded by a contractile sheath[8]. This contains protein subunits arranged in successive annuli which are rotated with respect to one another, so that the subunits also lie along oblique helical lines. On injection of the phage DNA into the host cell the sheath contracts, riding up the core. By comparing extended and contracted sheaths, we hope to discover the path of the contraction process.

Fig. 1 shows an electron micrograph of an extended phage tail which has been negatively stained. Its optical diffraction pattern, reproduced in Fig. 2, is essentially symmetrical about the meridian; because the tail is helical, this shows that the micrograph is made up by superposition from equally contributing substructures at the near and far sides of the particle[1]. The diffracted rays from the unwanted side of the particle can now be filtered out, and a good image of the other side obtained by optical recombination of the remaining diffracted rays[2]. Fig. 3 shows such an image from one side of the phage tail, but the picture is still complex, because it contains detail coming from different radii of the particle. This difficulty is overcome by our new reconstruction method which allows us to work in three dimensions and thus to separate the various radial contributions§.

Fig. 5 shows a model of the phage tail, consisting of the core together with its sheath, obtained by application of this method to the image in Fig. 1. It represents a Fourier synthesis of the particle at a resolution of 35 Å, in which the solid parts represent regions inaccessible to the negative stain. Comparison of such density maps from four different particles revealed only slight differences. The model contains two sets of black wires threaded through the two most prominent helical grooves; they form parallelograms which mark out the unit cells. There are six unit cells spanning the equator of the particle, corresponding to the number of subunits in the annulus[10,11].

We find a hole of about 30 Å diameter along the axis of the particle as we move outwards from the centre. This is formed probably by the packing of protein subunits in the tail core about a rotational symmetry axis. The resolution, however, is not sufficient to show up any fine periodic variations in the surface bounding this hole*. The model does show strong azimuthal fluctuations in density at two radii. Six helical tunnels of about 30 Å diameter lie at a radius of 65 Å, corresponding to the boundary between the sheath and the tail core (Fig. 5c). The matter which alternates with the tunnels at this radius presumably represents the connexions between tail and core. (These are to be expected, since the sheath is found in the extended state only when surrounding a core. Free sheaths are always contracted[12].)

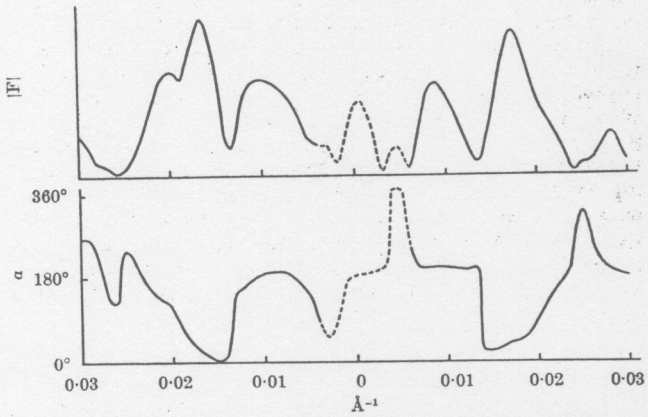

Fig. 4. Part of the computer-generated Fourier transform of the image of the tail in Fig. 1. The Fourier amplitude |F| along the second layer line is shown (compare Fig. 2), together with the accompanying phase α. The dotted parts of the curves near the middle of the diagram depend upon the exact region used to produce the Fourier transform; the regions used to produce this figure and Fig. 2 were not exactly the same.

A complex set of protuberances extends from a radius of about 90 Å to one of 120 Å at the outermost edge of the particle. They begin in the region of the model marked *L* (Fig. 5*a* and *b*) between the annuli, then sweep up to the right, as they pass through the region of an annulus, and finally join up by diagonal bridges (*S*) with the units on the upper left and lower right. The finer of the two sets of black wires near the surface passes under the bridges. The lower left-hand part of the protruding unit is almost in contact with the unit below and to the left. We cannot be sure, however, whether these units are really not in contact or whether we merely chose the contours marking the boundary between protein and stain at slightly too high a density.

Surprisingly, the cross-striations which give the appearance of annuli in the electron microscope are absent in the model. The cross-striations in the image are produced by the superposition of outer gaps and inner holes and do not correspond to deep serrations in the particle.

General Principles of Three Dimensional Reconstruction

Because of its high rotational symmetry, only a single two dimensional electron micrograph was needed to determine the three dimensional structure of the phage

* It should be stated that, in computing the map of the structure, it has been assumed that all the matter in the tail has the same symmetry. If the core had a different symmetry from the sheath, small modifications would be introduced into the model, but the main features described in this paper would be unchanged.

* Our method can be reformulated so as to carry out the reconstruction process without going through the intermediate stage of calculating Fourier coefficients, but this stage provides a useful point at which to check and if necessary correct the data. For example, in the case of a particle with helical symmetry like the phage tail, the relationship of the phases on the two sides of the meridian of a computer-generated Fourier transform provides a check that the axis of the particle has been correctly chosen (compare Fig. 4). If the axis were not quite correctly chosen, its position can be refined in Fourier space.

† For example, for a helical particle the three dimensional Fourier programme takes the form of a Fourier–Bessel synthesis into which the appropriate helical parameters can be inserted[9].

‡ The parallel with X-ray diffraction can be carried further, for it is possible to determine the Fourier amplitudes by optical diffraction from the electron microscope images. The determination of phases optically is more difficult, but we have tried out two optical techniques for phase determination. (1) The straightforward, but tedious, method in which diffracted rays are allowed to interfere pairwise to produce fringes, the positions of the fringe minima with respect to some reference point giving the phase. The procedure was carried out on our optical filtering system (compare ref. 2), but is very laborious and was less accurate than the densitometry method. (2) A holographic method in which the diffracted rays from the subject are allowed to interfere with a strong reference beam coming from a point in the same plane as the subject. The holographic technique using this particular geometry has been variously termed "Fraunhofer diffraction holography"[4] and "Fourier transform holography"[5]. This method has the same basis as the heavy-atom method in X-ray crystallography[6]. The method was not pursued intensively, because our first trials showed that, with subjects such as ours containing very fine detail, a proper interferometric system would have to be constructed[7].

§ Optical filtering is basically a two dimensional operation and gives direct results when applied to structures which are essentially two dimensional, such as overlapping sheets[3], thin-walled tubes (our work in preparation on the structure of the polyheads of bacteriophage *T4*; Kiselev, N. A., De Rosier, D. J., and Klug, A., work in preparation on the structure of tubes of catalase) or shallowly grooved solid objects (compare ref. 2).

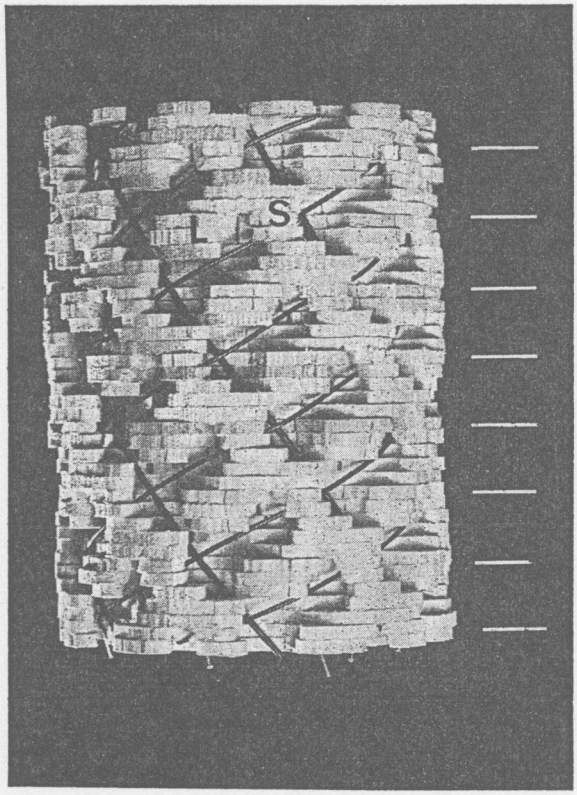

a

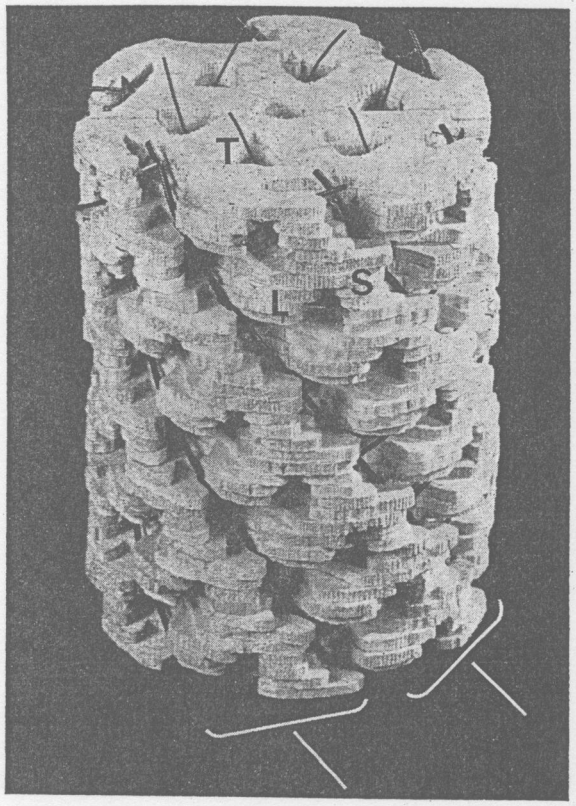

b

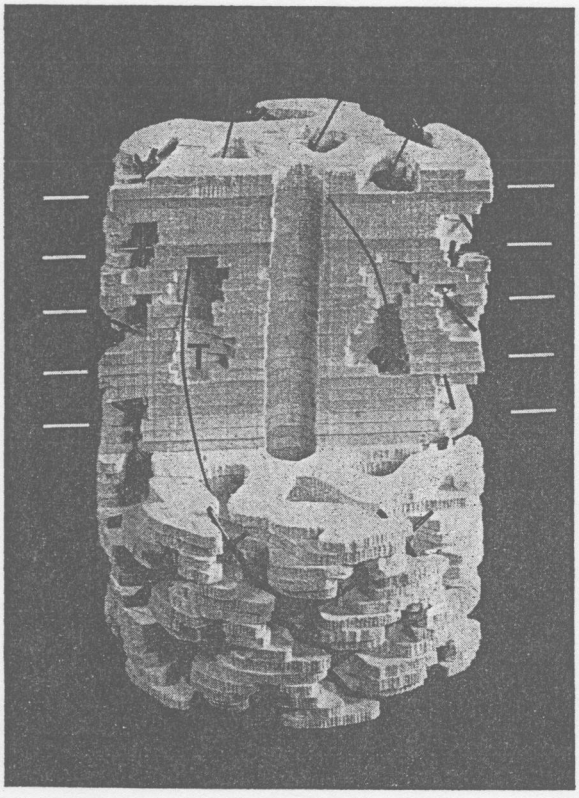

c

Fig. 5. Model of the phage tail in the extended state. The portion shown is about one-third of the actual length. The model was built from a series of sections in a three dimensional Fourier density map which includes data to spacings of 35 Å. *a*, Side view. The black wires lying in the prominent helical grooves on the surface serve to mark out the unit cells of the repeating structure. The horizontal lines at the side of the photograph mark the position of the annuli of subunits which can be seen in the electron micrograph in Fig. 1. *b*, Model tilted forward. The fine black wires *T* follow the path of the helical tunnels at an inner radius of about 60 Å. *c*, Same as *b*, but with part of the front half removed. The helical tunnels *T* lie between the tail core and the sheath.

The six pronounced helical ridges on the surface which run at an angle of about 30° to the particle axis (marked by brackets in *b*) can be identified with the helical "windings" which have been revealed at the surface by shadowing with metal[13]. This identification fixes the absolute hand of this family of helices. The same family of helices can be seen as the stronger of the two sets of oblique lines in the filtered image in Fig. 3, but their apparent hand is reversed there because it is the filtered image corresponding to the far side which is shown.

tail. We now outline the conditions for the recovery of any type of three dimensional structure from transmission photographs and we formulate the part played by symmetry more precisely. Large objects are examined usually by taking electron micrographs of thin sections, but this is not possible for small particles. Instead of working with the particle directly, however, equivalent structural information in the form of its Fourier amplitudes and phases can be used. If these could be measured in three dimensions, they could be used in a Fourier synthesis to compute the structure itself.

The electron microscope image represents a projection* of the three dimensional density distribution in the object at all levels perpendicular to the direction of view. According to a theorem familiar to crystallographers, the Fourier coefficients calculated from a projection of a three dimensional density distribution form a section through the three dimensional set of Fourier coefficients corresponding to that distribution. By collecting many different projections of a structure in the form of electron microscope images, it should therefore be possible to collect, section by section, the full set of Fourier coefficients required to describe that structure (Fig. 6). The number of projections needed to fill Fourier space roughly uniformly depends on the size of the particle and on the resolution, in much the same way as the number of zero-layer precession photographs in a three dimensional X-ray analysis depends on the unit cell size and the desired resolution. Similarly, rotation or screw symmetry reduces the number of sections required, because different orientations of the particle present identical projections†. The advantage of symmetry is illustrated in Table 1 which gives the number of independent views required to solve, to a resolution of about 30 Å, comparable structures of linear dimensions of about 250 Å.

Table 1

Symmetry class	Example	No. of views
Helical	*T*4 phage tail	1
Icosahedral	Tomato bushy stunt virus	~2
No symmetry	Ribosome	~30

It may be helpful to restate the role of symmetry differently. The projection of an object with rotational symmetry is the sum of projections of its asymmetric unit in the various symmetry-related orientations (and positions). In the reconstruction process the three dimensional structure of the asymmetric unit is recovered from the various projections of it which are contained in a single image of the whole object. Looked at in this way, an electron microscope image of the phage tail, which has forty-two subunits in its axial repeat, effectively presents projections of the subunit in twenty-one different orientations, more than enough to reconstruct the structure‡. The simplicity introduced by the symmetry of the phage tail made us choose it for our first attempt at three dimensional electron microscopy.

At this point, it is worth discussing the reason why high-resolution stereo-electron microscopy is not, in general, an adequate technique for solving a structure. Stereo-microscopy does not reproduce structures in a quantitative and tangible form, and has other drawbacks. Information from pairs of corresponding points in a stereo-pair is combined visually. Even if one had ideal pictures in which point-like features were clearly resolved, some points in a complex, deep structure would probably be obscured by others in front of them. To overcome this difficulty, many pairs of stereo-pictures would have to be taken. This brings one back to the requirements discussed above, but the procedure does not tell one how these views might be combined, even subjectively. For these reasons, stereoscopy is only suitable for seeing details confined to the neighbourhood of a single surface or for particularly simple three dimensional objects.

General Requirements for Implementation

If more than one projection of an object is needed to resolve its structure, such projections can be obtained in two ways. The most obvious one is to systematically tilt

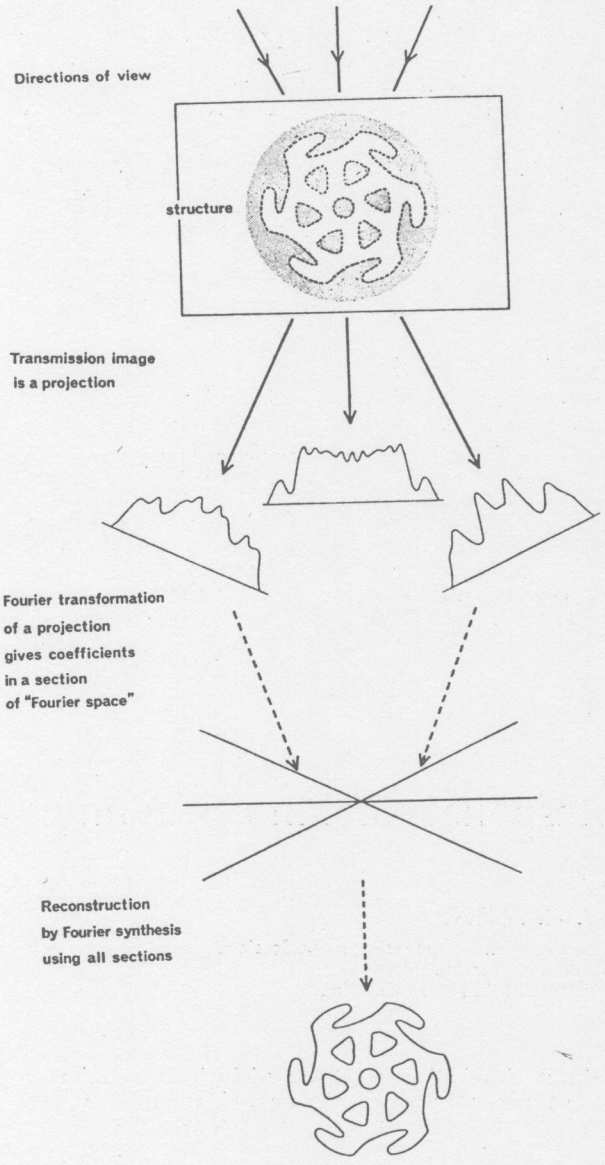

Fig. 6. Scheme for the general process of reconstruction of a structure from its transmission images.

* In precise terms, it is the logarithm of the intensity of the transmitted electron beam in the image which represents the projection of the three dimensional distribution of absorbing (strictly scattering) material along the path of the beam. For a distribution $\varrho(x, y, z)$, the transmitted intensity I is, in conditions of single scattering of electrons, related to the incident intensity I_0 by the expression $I(x, y) = I_0 \exp[-\mu \int \varrho(x, y, z)\, dz]$, where μ is the mass absorption coefficient and z is measured along the direction of the beam. This interpretation on a mass-thickness basis is, of course, only valid if the stain is amorphous[14], and if the spatial order in the liquid-like arrangement of scattering atoms is not shown up at the resolution with which one is concerned in the image[15]. This condition is obeyed for the scale of structure normally investigated in biological applications of electron microscopy. Likewise the condition of single scattering is obeyed for the thicknesses of stain involved.

For our quantitative work a measure of the transmitted electron beam is given by the optical density on the electron microscope plate which is proportional to it[16]. Thus in effecting the Fourier transformation of the electron microscope images, logarithms of the optical densities should be used to obtain the Fourier coefficients of the structure $\varrho(x, y, z)$. Taking the logarithm is easy in numerical processing, but presents a problem when optical methods are used to measure Fourier amplitudes and phases, for the logarithm of transmitted intensity in an optical system is directly proportional to the optical density and not to the logarithm of the optical density.

† This statement assumes that the distribution of stain possesses the particle symmetry (for example, it could have the form of a cylinder for a helical particle). Departures from this must be taken into account, and the technical problem will be discussed elsewhere.

‡ In terms of helical diffraction theory, the amplitude of the Fourier transform of the phage tail has cylindrical symmetry to the working resolution because there is no overlap of Bessel functions of different order on the layer planes[17].

and photograph a single particle in the electron microscope. If all the necessary projections are collected regardless of particle symmetry, no assumptions are needed to calculate the three dimensional structure. The synthesis will reproduce any symmetry that the particle possesses, but also any distortion it has suffered, or any irregularity in the stain distribution. These defects, however, can be detected by comparing Fourier syntheses of different particles. For a complete set of projections, the particles must be tilted accurately by small increments to a total tilt angle of 180°. This, however, presents the technical problems both of covering the complete range of angles and of preserving the structure during successive exposures to the electron beam. Symmetry lessens the difficulties by reducing both the number of different projections and the maximum tilt angle required. So that symmetry can be used, the orientations of the symmetry axes with respect to the tilt axes must be found.

Alternatively, different images from a field of particles are, in principle, projections of the same structure (although in practice allowance must be made for variations in staining or perturbations in the different particles). The exact orientation of each particle in relation to the direction of view must be determined in order to relate correctly the Fourier space section obtained from it to those obtained from other particles. This would mean determining the orientation of the particle for each image before its exact structure is known. In practice, ancillary tilting experiments would help in the recognition of the views[18,19]. Recognition and determination of the angle of view might be done more precisely by some form of refinement process, such as the simulation of particle images using a provisional model of the structure[18,19]. This would also help in assessing the preservation of detail in the different images. It is important to integrate the information contained in the images of different particles so that the effects of noise coming from the sources mentioned above can be averaged out.

Concluding Remarks

Our method of three dimensional reconstruction relates the analysis of electron microscope images to the theory that has been developed for X-ray diffraction analysis. The difference is that the "phase", which together with the amplitudes of the Fourier components allows the reconstruction of a three dimensional map, is lost in recording the X-ray diffraction data. It is preserved, however, by the focusing of the diffracted electron beam into an image. At the same time, one can work with a single or a few particles and one is not confined to working with highly ordered crystals or fibres as in protein crystallography. While small numbers of particles can be used, more variability must be expected than is encountered in the average structure from, for example, a protein crystal containing 10^{15}–10^{17} particles*.

Because the theory underlying this method is a very general one, the method can be used for all kinds of objects. It may be necessary, however, to modify the various procedures used according to the particular problem. In the example given here we have used single particles, but the method could work equally well with ordered aggregates or arrays such as sections of muscle or small crystals.

We thank Dr J. T. Finch for the electron micrographs, R. A. Crowther for programming the densitometer and for help with the computer processing, Dr K. C. Holmes for making his Fourier–Bessel programme available and Miss Marion Holder for technical assistance. We also thank Professor Gill and the manager of the Computer Centre, Imperial College of Science and Technology, for making facilities available. We thank Drs H. E. Huxley and M. F. Perutz for helpful criticism of earlier versions of this article. One of us (D. J. De R.) was aided by a grant from the American Cancer Society.

Received January 3, 1968.

* Because the preservation of detail in electron micrographs is not usually perfect, many examples must be examined and assessed. The method of optical diffraction[1] provides an objective assessment of the information contained in an image of a periodically repeating structure, for it displays an average of the genuine, repeating features. We have found by this technique that the resolution in electron micrographs of negatively stained biological specimens can be as high as 15–20 Å (refs. 1 and 2).

1 Klug, A., and Berger, J. E., *J. Mol. Biol.*, **10**, 565 (1964).
2 Klug, A., and De Rosier, D. J., *Nature*, **212**, 29 (1966).
3 Klug, A., Crick, F. H. C., and Wyckoff, H. W., *Acta Cryst.*, **11**, 199 (1958).
4 Leith, E. N., and Upatnieks, J., *J. Opt. Soc. Amer.*, **54**, 1295 (1964).
5 Stroke, G. W., *App. Phys. Lett.*, **6**, 201 (1965).
6 Bragg, W. L., *Nature*, **166**, 399 (1950).
7 Vander Lugt, A., *Trans. IREE*, IT-10, 139 (1964).
8 Brenner, S., Streisinger, G., Horne, R. W., Champe, S. P., Barnett, L., Benzer, S., and Rees, M. W., *J. Mol. Biol.*, **1**, 281 (1959).
9 Finch, J. T., Klug, A., and Nermut, M. V., *J. Cell Sci.*, **2** (December, 1967).
10 Moody, M. F., *J. Mol. Biol.*, **25**, 201 (1967).
11 Krimm, S., and Anderson, T. F., *J. Mol. Biol.*, **27**, 197 (1967).
12 See, for example, Kellenberger, E., and Boy de la Tour, E., *J. Ultrastruct. Res.*, **11**, 545 (1964).
13 Williams, R. C., and Fraser, D., *Virology*, **2**, 289 (1956).
14 Hall, C. E., *Introduction to Electron Microscopy*, ch. 9 (McGraw-Hill, New York, 1953).
15 Heidenreich, R. D., *Fundamentals of Transmission Electron Microscopy*, ch. 1 (Interscience, London, 1964).
16 Various contributions in *Symp. on Quantitative Electron Microscopy* (edit. by Bahr, G. F., and Zeitler, E. H.) (The Williams and Wilkins Company, Baltimore, 1965).
17 Franklin, R. E., and Klug, A., *Acta Cryst.*, **8**, 777 (1955).
18 Finch, J. T., and Klug, A., *J. Mol. Biol.*, **15**, 344 (1966).
19 Klug, A., and Finch, J. T., *J. Mol. Biol.* (in the press, 1968).

Response of Pine Seedlings to Mechanical Stimulation

by
W. C. ASHER
Southeastern Forest Experiment Station,
US Forest Service Research,
Triangle Park, North Carolina

When needles of pine seedlings are deflected downwards there is an electrical response which can be measured.

When developing electrophysiological techniques for forest tree physiology research, I observed a hitherto unreported electrical "response" to leaf fascicle movement in young slash (*Pinus elliottii* variety *elliottii* Engelm.) and loblolly (*P. taeda* L.) pine trees. The effect can be elicited consistently by sharply deflecting a fascicle downward while recording the electrical potential between two or more points on the stem of the tree with non-polarizing electrodes. The response is rapid and sharply defined and seems to be typical of tissue depolarization.